Astron. Astrophys. 319, 470–480 (1997)

ASTRONOMY
AND
ASTROPHYSICS

Globular cluster systems of early-type galaxies in Fornax⋆

M. Kissler-Patig[1,2], **S. Kohle**[2], **M. Hilker**[2], **T. Richtler**[2], **L. Infante**[3], **and H. Quintana**[3]

[1] European Southern Observatory, Karl-Schwarzschild-Str. 2, D-85748 Garching, Germany
[2] Sternwarte der Universität Bonn, Auf dem Hügel 71, D-53121 Bonn, Germany
[3] Departamento de Astronomía y Astrofísica, P. Universidad Católica, Casilla 104, Santiago 22, Chile

Received 20 May 1996 / Accepted 5 August 1996

Abstract. We studied through V and I photometry the properties of the globular cluster systems of five early-type galaxies in the Fornax galaxy cluster: NGC 1374, NGC 1379, NGC 1387, NGC 1427, and the central giant elliptical NGC 1399. While the four normal galaxies have between 300 and 500 globular clusters, leading to specific frequencies of 4 ± 1 for all of them, NGC 1399 has around 6000 ± 600 globular clusters and a specific frequency of 12 ± 3.

The globular cluster colors are somewhat redder than those of the Milky Way globular clusters, however with a similar dispersion. This indicates a wide range of metallicities in all our galaxies with a mean metallicity somewhat higher than in the galactic halo, comparable to the galactic bulge. In NGC 1399 the dispersion is about twice as high, and the color distribution could be multi-modal. No color gradient could be detected within the sensitivity of our photometry.

The density profiles of the globular cluster systems follow the galaxy light in all the galaxies. In NGC 1399 the globular cluster system is much flatter than in the other galaxies, but coincides with the large cD envelope of the galaxy. None of the globular cluster systems is clearly elongated, even the ones in NGC 1374 and NGC 1427 (E1 and E3 respectively) appear rather spherical.

From a comparison with studied globular cluster systems in spiral galaxies, we conclude that our faint ellipticals have no more globular clusters than spirals of the same mass, and neither differ in their other properties, such as globular cluster colors and morphological properties of the system. For these galaxies there is no need to imply a different formation scenario of the globular cluster system. The central giant elliptical has far more globular clusters and shows signatures of a different history in the building up of its globular cluster system.

Key words: galaxies: clusters: individual: Fornax – galaxies: elliptical – galaxies – star clusters – globular clusters: general

Send offprint requests to: M. Kissler-Patig (Bonn)

⋆ Based on data collected at the Las Campanas Observatory, Chile, run by the Carnegie Institutions

1. Introduction

The study of globular cluster systems around galaxies beyond the Local Group has become routine (Harris 1991, Richtler 1995). Around 70 galaxies and their systems have been investigated to date (Harris & Harris 1996). Several systematics have been identified, but none of them was yet fully understood with respect to the galaxy history. The probably most controversial point is the number of globular clusters and the specific frequency S (number of globular clusters per galaxy luminosity in units of $M_V = -15$ mag). While the discrepancy of the S values between spirals and ellipticals was used as an argument against a scenario where ellipticals were built up by mergers (e.g. Van den Bergh 1990), other authors (e.g. Ashman & Zepf 1992) suggested that the problem might be solved by globular clusters being formed during the merging events as seen in several galaxies (NGC 3597: Lutz 1991; NGC 1275: Holtzman et al. 1992; NGC 7252: Whitmore et al. 1993, Schweizer & Seitzer 1993; He 2-10: Conti & Vacca 1994; NGC 4038/4039: Whitmore & Schweizer 1995; NGC 5018: Hilker & Kissler-Patig 1996). However it is still uncertain if globular cluster formation in interactions was effective enough (e.g. Harris 1995) to explain the apparently higher number of globular clusters in ellipticals compared to spirals.

We investigate here a sample of five early-type galaxies in the Fornax galaxy cluster. Our target galaxies are NGC 1374, NGC 1379, NGC 1387, NGC 1427, and the central giant cD galaxy NGC 1399. The globular cluster luminosity functions have been presented in Kohle et al. (1996, hereafter Paper I). Earlier photographic work already exists for these galaxies (Hanes & Harris 1986) and provides a basis for comparison. The globular cluster system of NGC 1399 has been investigated by several authors (Geisler & Forte 1990, Wagner et al. 1991, Bridges et al. 1991, Ostrov et al. 1993), to which we will refer later on. General data of our galaxies are summarized in Table 1. We investigated the number of globular clusters (Sect. 3), the colors and color distributions (Sect. 4), as well as the radial and spatial distribution of the globular clusters (Sect. 5). Our conclusions are presented in Sect. 6.

Table 1. General data of our target galaxies, all members of the Fornax galaxy cluster, taken from Tully (1988), Poulain (1988), and Poulain & Nieto (1994)

name	RA(2000)	DEC(2000)	l	b	type	m_V	$(V-I)$	V_0[km s^{-1}]
NGC 1374	03 35 16	-35 13 35	236.36	-54.29	E1	11.20	1.20	1105
NGC 1379	03 36 03	-35 26 26	236.72	-54.13	E0	11.20	1.19	1239
NGC 1387	03 36 57	-35 30 23	236.82	-53.95	S0	10.81	1.30	1091
NGC 1399	03 38 29	-35 26 58	236.71	-53.64	E0	9.27	1.25	1294
NGC 1427	03 42 19	-35 23 36	236.60	-52.85	E3	11.04	1.15	1416

Table 2. The log of our observations: all exposures were approximately centered on the galaxies, except for NGC 1399, which was covered by a 4 image mosaic. We used a Bessell V and Kron-Cousins I filter. The seeing is quoted as measured from the FWHM of stellar object on the images

Galaxy	Filter	Obs. date	Exposure time	seeing
NGC 1374	V	28.9.94	2×1200s	1".2
	I	29.9.94	1200s +2 $\times$ 600s	1".5
NGC 1379	V	29.9.94	2×1200s	1".2
	I	26.9.94	3×1200s	1".4
NGC 1387	V	28.9.94	2×900s	1".3
	I	28.9.94	2×900s	1".2
NGC 1427	V	26.9.94	3×1200s	1".5
	I	26.9.94	3×1200s	1".3
NGC 1399	V	27.+28.9.94	2×900s / field	1".0
	I	27.+28.9.94	2×900s / field	1".2

Table 3. Calibration coefficients for our different nights. Column 5 lists the RMS of the difference between our standard magnitudes and our calibrated ones

night	$v1$	$v2$	$v3$	RMS
26.9.	$1.718 \pm .018$	$0.100 \pm .012$	$-0.019 \pm .007$	0.020
27.9.	$1.671 \pm .009$	0.133 fixed	$-0.020 \pm .009$	0.024
28.9.	$1.713 \pm .018$	$0.101 \pm .012$	$-0.018 \pm .007$	0.020
29.9.	$1.668 \pm .009$	0.133 fixed	$-0.020 \pm .009$	0.024
night	$i1$	$i2$	$i3$	RMS
26.9.	$2.077 \pm .012$	$0.038 \pm .008$	$-0.013 \pm .005$	0.012
27.9.	$2.065 \pm .005$	0.047 fixed	$-0.017 \pm .005$	0.011
28.9.	$2.069 \pm .016$	$0.041 \pm .010$	$-0.006 \pm .007$	0.013
29.9.	$2.066 \pm .007$	0.047 fixed	$-0.015 \pm .006$	0.015

2. Observations and reduction

2.1. The observations

The data were obtained in the nights of 26-29 September, 1994 at the 100 inch telescope of the Las Campanas observatory, Chile, run by the Carnegie Institution. We used a Tektronix 2048×2048 pixel chip, with a pixel size of 21μm or $0\farcs227$ at the sky, corresponding to a total field of view of $7\farcm74 \times 7\farcm74$. The chip was operated with a readout noise of $8.3e^-$, and a gain of $3.1e^-$/ADU.

The observations of the different galaxies are detailed in Table 2. In addition to the long exposures, we obtained several 60-second exposures in both filters centered on all the galaxies. The SE and SW fields around NGC 1399 will not be considered in the following: several I exposures of the SW field were corrupted, while the SE field includes part of NGC 1404 (another member of Fornax), which makes the allocation of globular clusters to the one or the other galaxy confusing.

2.2. The reduction

All reductions were done in IRAF. Bias frames were subtracted and sky flat-fields of different nights were averaged to flatten the images better than 1%. The different long exposures were then combined with a sigma clipping algorithm, to remove the cosmetics from the final frames.

Object search, photometry, and the determination of the completeness factors were done with the DAOPHOT II version in IRAF. For all galaxies we computed an isophotal model in each filter (using the STSDAS package *isophote*) that we subtracted from our final long exposure to obtain a flat background for the object search and photometry.

The nights of the 26, 27 and 29 were photometric and the calibration was done via typically 15-30 standard stars from the Landolt (1992) list, taken throughout the nights, by which our Bessell V colors were transformed to Johnson V. In the middle of the night of the 28^{th} cirrus passed. Frames taken at that time were calibrated via aperture photometry on the galaxy published by Poulain (1988), and Poulain & Nieto (1994) and cross-checked with overlapping frames in the case of NGC 1399. All other calibrations were also inter-compared and found compatible with the aperture photometry values for the individual galaxies. Table 3 shows our final coefficients for the calibration equations:

$V_{inst} = V + v1 + v2 \cdot X_V + v3 \cdot (V-I)$

$I_{inst} = I + i1 + i2 \cdot X_I + i3 \cdot (V-I)$

where instrumental magnitudes are normalized to 1 second and given with an offset of 25 mag.

The completeness calculations were done by standard artificial star experiments. We added typically 10000 stars over many runs on a long exposure and repeated the reduction steps starting with the object finding. The completeness values are given in detail in Fig. 1 of Paper I. The completeness limit of 50% is reached at $V \simeq 23.5$ mag, $I \simeq 22.5$ mag for our four normal galaxies, 0.5 mag deeper for the NE and NW fields (fields 2 and 4 in Paper I) around NGC 1399.

Table 4. Number of globular clusters around our target galaxies. Column 1 lists the name of the galaxy, column 2 the background corrected counts down to the turn-over of the GCLF together with the errors from the background correction and the error in the assumed turn-over. The measured turn-over value of the GCLF is shown in column 3, column 4 and 5 list the uncovered area towards the center of the galaxies and the correction, column 6 lists the correction for the area beyond 120″ from the center, column 7 and 8 give the total amount of globular clusters within 120″ and around the galaxy

Galaxy	raw counts	turn-over	geom. correct.		correct. $>120''$	total $<120''$	**total**
counts from the GCLF in V							
NGC 1374	$118 \pm 15 \pm 11$	23.52 ± 0.14	0.072	5.4 ± 3.6	156 ± 72	248 ± 38	404 ± 81
NGC 1379	$114 \pm 15 \pm 24$	23.68 ± 0.28	0.091	6.8 ± 4.6	51 ± 19	245 ± 57	296 ± 60
NGC 1387	$143 \pm 07 \pm 31$	23.80 ± 0.20	0.450	34 ± 23	24 ± 10	365 ± 110	389 ± 110
NGC 1427	$166 \pm 19 \pm 21$	23.78 ± 0.21	0.072	5.4 ± 3.6	189 ± 66	344 ± 58	533 ± 88
NGC 1399 NE	$539 \pm 19 \pm 43$	23.90 ± 0.08	see text		–	–	6270 ± 640
NGC 1399 NW	$525 \pm 19 \pm 38$	23.90 ± 0.08	see text		–	–	5960 ± 600
counts from the GCLF in I							
NGC 1374	$124 \pm 11 \pm 17$	22.60 ± 0.13	0.072	5.4 ± 3.6	156 ± 72	259 ± 41	415 ± 83
NGC 1379	$133 \pm 11 \pm 29$	22.54 ± 0.34	0.091	6.8 ± 4.6	51 ± 19	280 ± 63	331 ± 66
NGC 1387	–	–	–	–	–	–	–
NGC 1427	$143 \pm 10 \pm 13$	22.31 ± 0.13	0.072	5.4 ± 3.6	189 ± 66	297 ± 56	486 ± 87
NGC 1399 NE	$457 \pm 16 \pm 19$	22.27 ± 0.05	see text		–	–	5460 ± 505
NGC 1399 NW	$537 \pm 16 \pm 24$	22.27 ± 0.05	see text		–	–	6070 ± 520

3. The number of globular clusters

3.1. Globular cluster counts

We computed the number of globular clusters present down to the turn-over of the globular cluster luminosity functions (GCLF) presented in Paper I for each galaxy. We then corrected these counts for a possible incompleteness in the area covered, using the density profiles of Sect. 5.2. We assumed the GCLF to be symmetric around the turn-over and doubled our counts to get the total number of globular clusters in the galaxies.

For all the galaxies, except for NGC 1399, the counts for the globular cluster luminosity function were computed in an area extending out to 120″ radius (about 10 kpc at the distance of Fornax). The density profiles in Sect. 5.2 show that the density of globular clusters reaches the background at about this radius in NGC 1379 and NGC 1387, but extends further in NGC 1374 and NGC 1427. Geometrical corrections had therefore to be applied for the non-covered areas in the center of the galaxies (see columns 4 and 5 in Table 4), as well as for the region beyond 120″ from the center of the galaxies (column 6 in Table 4). The latter correction was computed by subtracting the respective mean background densities (see Sect. 5.2) from the object densities in Table 7, then summing the number of globular clusters in the outer rings after correction for completness. For the central regions of the galaxy, we extrapolated the density profiles inwards taking into account that the density in a globular cluster system does not rise steeply towards the center (e.g. Aguilar et al. 1988) and assumed a density of 75 ± 50 globular clusters per square arcmin down to the turn-over in the inner, uncovered regions of all four galaxies.

For NGC 1399, we individually computed the counts on our NE and NW fields from 1.0′ to 9.5′ radius. The NE fields holds 20.1%, the NW field 20.8% of this ring and includes the center of the galaxy. For the inner region we assumed a mean density of 100 ± 50 globular clusters per square arcmin down to the turn-over (see the density profiles in Sect. 5.2), thus 560 ± 280 objects over the 2.8 square arcmin for the full GCLF. Further we estimated the globular cluster system to extend out to about 12′ (see also Hanes & Harris 1986), with a mean density of 1 ± 1 globular clusters per square arcmin down to the turn-over beyond 9.5′ thus 340 ± 340 globular clusters over the full GCLF in the uncovered outer region. From both the NE and NW field we then extrapolated the total number of globular clusters around the whole galaxy and got consistent results.

The results are summarized in Table 4 with the following sources of errors taken into account. The number of globular clusters were computed in Paper I as the excess objects around the galaxies, and thus affected by the uncertainties of the background determination (square root of the background counts) and of the turn-over value. The counts down to the turn-over with their errors are shown in column 2, the assumed turn-over stands in column 3.

These total numbers compare well with the results of the photographic work of Hanes & Harris (1986) who found very similar raw counts down to their limiting magnitudes of B_j = 23.40-23.95. For NGC 1399, the various older works that determined the number of globular clusters (Wagner et al. 1991, Bridges et al. 1991) assumed larger distances for the Fornax cluster, and thus extrapolated their luminosity functions to larger total numbers. However their counts to their limiting magnitudes agree with ours.

3.2. The specific frequency

To derive the specific frequency (number of globular clusters per unit galaxian luminosity in units of $M_V = -15$) we determined the distance of the galaxies from their GCLF turn-over magnitudes. We computed the mean of the distance moduli derived in V and I, assuming an absolute turn-over magnitude

Table 5. Specific frequency for our target galaxies. Column 1 lists the name of the galaxy, column 2 the derived distance modulus, column 3 the absolute magnitude in V, column 4 the total number of globular clusters N_t, column 5 the specific frequency S_N

Galaxy	$(m-M)$	M_V	N_t	S_N
NGC 1374	$31.0 \pm .2$	$-19.8 \pm .2$	410 ± 82	4.9 ± 1.3
NGC 1379	$31.1 \pm .2$	$-19.9 \pm .2$	314 ± 63	3.4 ± 0.9
NGC 1387	$31.0 \pm .2$	$-20.2 \pm .2$	389 ± 110	3.2 ± 1.1
NGC 1427	$31.0 \pm .2$	$-20.0 \pm .2$	510 ± 87	5.1 ± 1.3
NGC 1399	$31.0 \pm .2$	$-21.7 \pm .2$	5940 ± 570	12.4 ± 3.0

of $V_{TO} = -7.4 \pm 0.2$ and $I = -8.5 \pm 0.2$ (see Paper I). The absolute magnitudes of the galaxies (see Table 1) were then combined with the total number from the previous subsection using the mean of the counts in V and I. The results are shown in Table 5.

NGC 1374, NGC 1379, NGC 1387, and NGC 1427 have specific frequencies around 4.0, while NGC 1399 deviates from that mean with $S_N = 12.4 \pm 3.0$. Again this is in agreement with the previous works. Hanes & Harris (1986) gave various values of S_N in function of the distance to Fornax (affecting both their counts and the luminosity of the galaxies) of around 4 for NGC 1374, NGC 1379, and NGC 1387. For NGC 1399 their values range from 11 to 19. Wagner et al. (1991) quoted a value of 15.4 ± 3.2 for NGC 1399, Bridges et al. (1991) a value of 16 ± 4. An interpretation will be given in the discussion.

4. The colors of the globular cluster systems

In this section we analyze the colors of the globular clusters around our galaxies. Globular clusters were selected in the same manner as for the GCLF, i.e. by the second moments of the intensity, as well as by the SHARP and CHI value returned from DAOPHOT. Most background galaxies (the main source for contamination) have outstanding values in at least one of these parameters, and could be removed.

4.1. The color distributions in the normal galaxies

We again considered only objects closer than $120''$ to the center of the respective galaxy in the case of our four normal galaxies. The color distribution of all the globular clusters around NGC 1374, NGC 1379, NGC 1387, and NGC 1427 are shown in Fig. 1. The same distribution for globular clusters that have errors in $V-I$ less than 0.1 mag (typically occurring between V = 22.5 mag and V = 23.0 mag) are shown in Fig. 2, in which we over-plotted two curves:

• the best fitting gaussian (solid line), which returned widths of σ = 0.11 to 0.13 mag.

• the expected distribution (dotted line) if all globular clusters would have the same color, and the broadening would be due to the errors of the photometry alone.

The narrow dispersions of our free gaussian fits show that the *intrinsic* dispersion of the distributions must be less than 0.1 mag. We performed the KMM test proposed by Ashman et al. (1994),

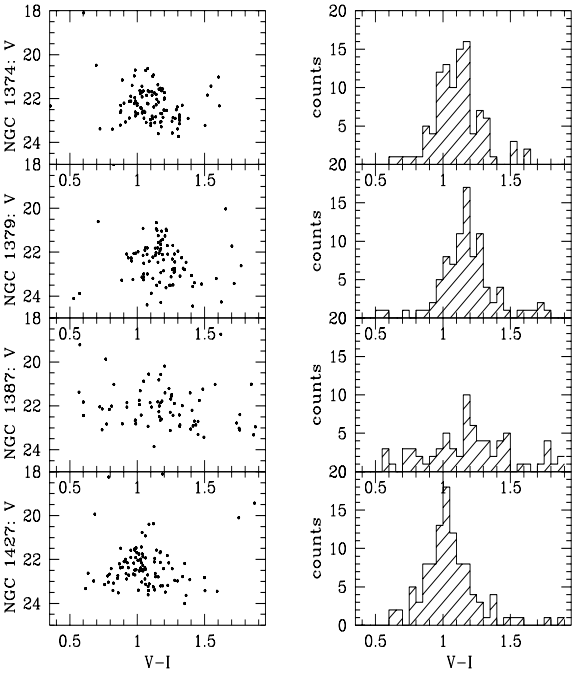

Fig. 1. The color distribution of all globular clusters around our galaxies. On the left our color magnitude diagrams, on the right the corresponding histograms with all globular clusters included

as well as fits with multiple gaussians, in order to detect multimodality in the distributions, but in no case the hypothesis of an unimodal distribution could be rejected.

While the width of the distribution is almost identical for these four galaxies, the median color slightly differs. We assumed $E(B-V) = 0.0$ towards Fornax (Burstein & Heiles 1982), and derived median $(V-I)$ colors of the globular clusters shown in Table 6, together with a median metallicity.

Deriving metallicities from broadband colors is complicated by second parameter effects: age and metallicity can hardly be disentangled. For similar ages and metallicities, the $V-I$ color of galactic globular clusters spread over about 0.2 mag.

From the relatively red ($V-I > 0.8$) mean colors, the quite narrow color distributions, the fact that we see no peculiarities in the luminosity functions of the globular clusters, and that there is no sign for any recent mergers, we are encouraged to assume that the globular clusters in these four galaxies are older then 10 Gyr. With this assumption on age we can roughly convert our colors to metallicities using the empirical color-to-metallicity relation found for the Milky Way globular clusters.

We updated the color-metallicity relation given in Couture et al. (1990), using the Mc Master catalogue (Harris 1996) of Milky Way globular clusters. Fig. 3 shows the metallicity of all the galactic globular clusters with a reddening $E(B-V)$ less than 0.4 (60 candidates) plotted against their $(V-I)_0$ color, that we corrected for extinction assuming $E(V-I) = 1.38 \times E(B-V)$ (Taylor 1986). The best linear fit gives the relation:
$(V-I)_0 = 0.15(\pm 0.02)$[Fe/H] + $1.13(\pm 0.03)$
This is valid, strictly speaking, only in the range $0.7 < (V-I) <$

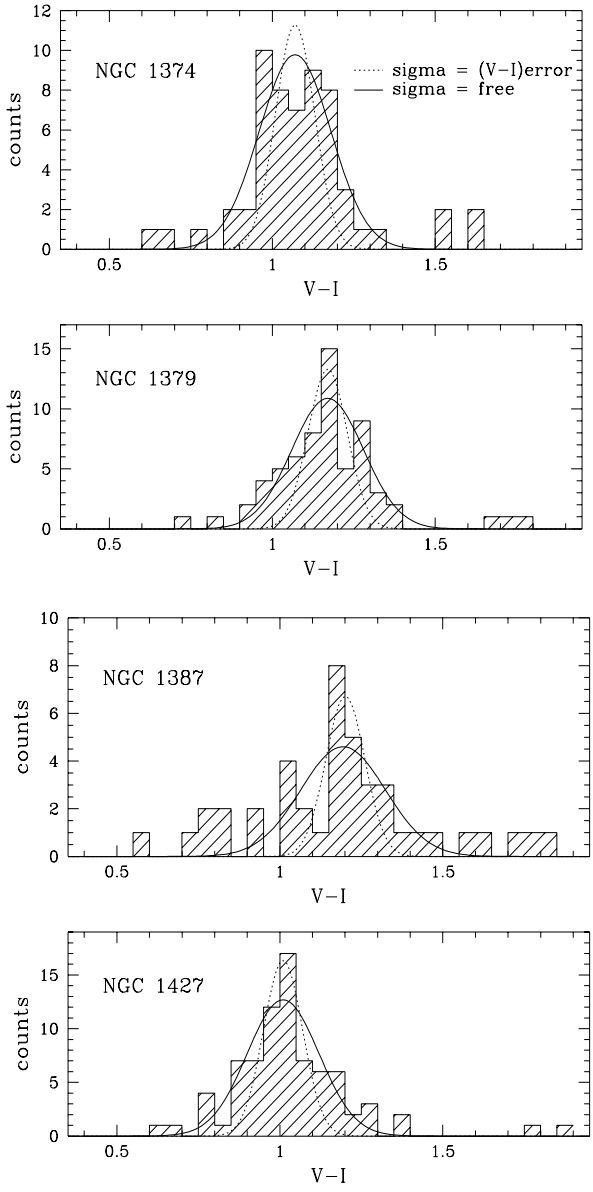

Fig. 2. Histogram of the globular cluster color distribution in $(V-I)$ around NGC 1374, NGC 1379, NGC 1387, and NGC 1427. The solid line is the gaussian fit to the distribution, the dotted one shows the broadening from the errors in $(V-I)$ alone

1.1. A direct comparison to the colors of the globular clusters in the Milky Way is also of interest. The color distribution of all the globular clusters in the Milky Way is shown in Fig. 4, the contribution of halo and bulge globular clusters are overplotted (dashed and black). A gaussian fit to the histogram leads to a mean value of $(V-I) = 0.90 \pm 0.01$ and a dispersion of $\sigma = 0.065 \pm 0.003$. This is comparable to the *intrinsic* dispersion of the color distributions of our galaxies, and corresponds to a range of metallicity from $[Fe/H] = -2.4$ to 0.2 dex.

Thus, from the colors alone, accurate metallicities cannot be derived, but we can conclude that:

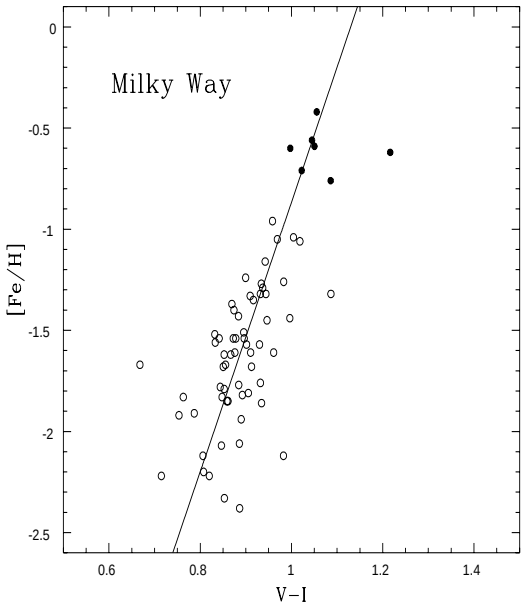

Fig. 3. Metallicity versus $(V-I)$ color for the globular clusters in the Milky Way with $E(B-V) < 0.4$. Dots are bulge clusters, circles are halo clusters, the line shows the best linear fit

Table 6. Median $V-I$ colors of the globular clusters around NGC 1374, NGC 1379, NGC 1387, and NGC 1379; as well as derived median metallicities

Galaxy	median $(V-I)$	[Fe/H]
NGC 1374	1.10 ± 0.03	-0.2 ± 0.3
NGC 1379	1.17 ± 0.03	0.3 ± 0.3
NGC 1387	1.20 ± 0.06	0.5 ± 0.4
NGC 1427	1.03 ± 0.03	-0.7 ± 0.3

- All our early-type galaxies have median colors of their globular clusters redder than that of the Milky Way. Assuming old globular cluster populations, this would mean average metallicities of the globular clusters ranging from slightly richer than the Milky Way halo (for NGC 1427) to about solar (for NGC 1379 and NGC 1387).
- There is no clear evidence for multiple populations, the range of metallicities for the globular clusters in each galaxy could span 2 dex in [Fe/H] as in the Milky Way, but is concentrated around a median value.
- The median color for globular clusters in all the galaxies is bluer by about 0.1 mag in $(V-I)$ than the integrated galaxy light, as already noticed in all galaxies observed up to date, but all our galaxies possess also globular clusters as red as the galaxy itself.

4.2. The globular cluster colors in NGC 1399

For NGC 1399 we considered all the globular clusters in the NE and NW fields obeying our selection criteria. Fig. 5 shows the color distribution of the globular clusters with errors in $V-I$ less than 0.1 mag. Here the best gaussian fit returns a width

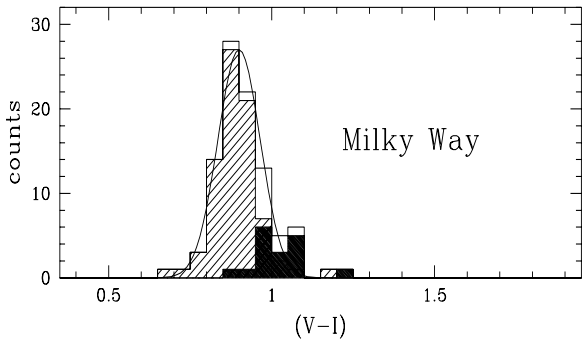

Fig. 4. Histogram over the $(V-I)$ color of the globular clusters in the Milky Way. The dashed region marks the contribution of the halo clusters, the black ones that of the bulge

of $\sigma = 0.22$, three times as large as expected from the errors only. For the sample composed by all globular clusters in the NE and NW field the KMM test rejects the unimodal hypothesis (with a confidence over 95%) if we impose dispersions of the color distributions comparable to the dispersions observed in our normal galaxies ($\sigma \simeq 0.12$), and favors two populations centered on $V-I = 0.99$ and $V-I = 1.18$ (corresponding to [Fe/H]= -0.9 and 0.3 dex according to our relation in the previous section). We note that the globular clusters do not span a much wider range of colors than in the other galaxies, but rather populate all colors more homogeneously, i.e. they are no globular clusters with peculiar colors in NGC 1399 compared to the other galaxies.

From Washington photometry Ostrov et al. (1993) also derived multiple peaks in the color distribution. They find two groups, at [Fe/H]= -1.5 and -0.9, as well as a possible third group near -0.2 dex. The shift in the color to metallicity conversion between our results demonstrates how difficult metallicity estimates are from broad band colors alone. The results from Washington photometry are probably more reliable than from the less metal sensitive V, I colors. The main result here is the confirmation of at least two groups of globular clusters in the color distribution.

This would suggest that two or more distinct globular cluster enrichment or formation epochs/mechanisms happened in NGC 1399.

4.3. A composite color distribution

As an experiment we constructed an artificial color distribution with all globular clusters found around NGC 1374, NGC 1379, NGC 1387, and NGC 1427 with errors in $V-I < 0.1$ mag. This is equivalent to the sum of the four histograms shown in Sect. 4.1.

The resulting composite color distribution is shown in Fig. 6. We performed the same test on it as for the other distributions: a single gauss fit returns a width of $\sigma = 0.31$; the KMM test favors a double gauss fit with 99% confidence if we impose individual width of $\sigma = 0.12$. This color distribution would probably be classified as **bi-**modal, in case of real data,

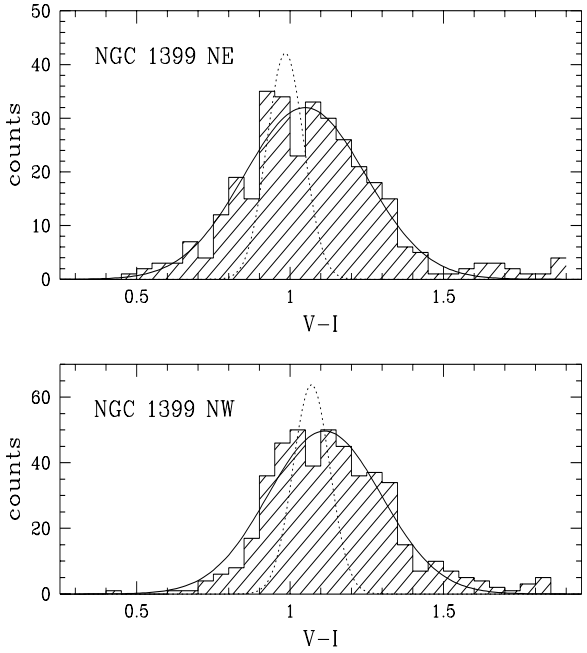

Fig. 5. Color distributions for the globular clusters in the NE (upper panel) and NW (lower panel) fields around NGC 1399. The solid line is a free gaussian fit and returns a dispersion of 0.22, while the dotted line shows the broadening expected from our errors in photometry alone

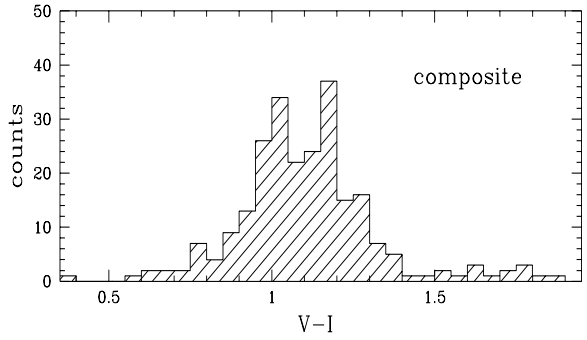

Fig. 6. Composite histogram of the $(V-I)$ colors of all the globular clusters with a $V-I$ error less than 0.1 mag in NGC 1374, NGC 1379, NGC 1387, and NGC 1427. The distribution seems to be bi-modal but is based on four systems

while it is composed of **four** globular cluster systems. We take it as a word of caution, that broad and multi-modal color distribution might hide a much more complex history than a single merger event between two galaxies, as Ashman & Zepf (1992) propose in a first approximation.

4.4. Color gradients

We present the radial color distributions of the globular clusters in Fig. 7. The globular clusters plotted are the same as used for the color distributions in the sections above, i.e. objects that match our criteria for point like sources have an error in $V-I$ of less than 0.1 mag, and are closer than 120″ (425″ in the case of

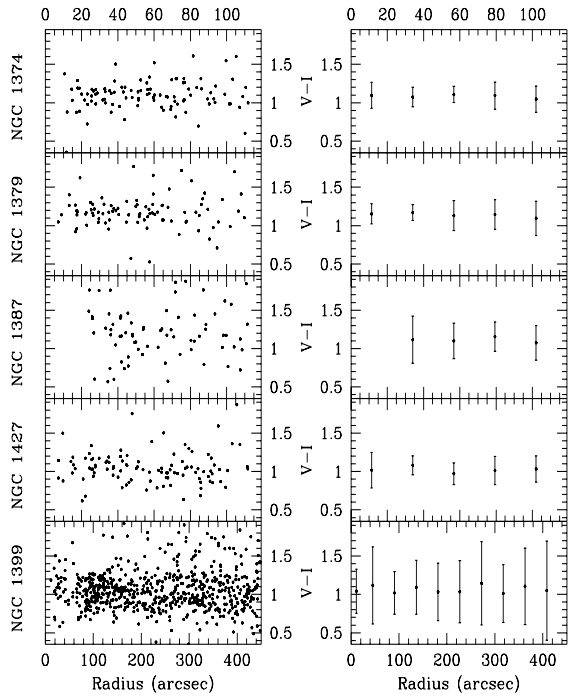

Fig. 7. Color gradients for our five target galaxies. Plots extend to 120″ for NGC 1374, NGC 1379, NGC 1387, and NGC 1427; to 425″ for NGC 1399. Errorbars show the dispersion around the median

NGC 1399) to the center of the parent galaxy. Color gradients in globular cluster systems is a topic of much debate. Where they are found, such gradients are small, typically of the order of 0.1 to 0.3 mag in common broad band indices over hundreds of arcseconds radius (e.g. in M87, Lee & Geisler 1993, in M49 and NGC 4649, Couture et al. 1991, in NGC 3923 Zepf et al. 1995, or in NGC 3311 Secker et al. 1995). For most galaxies where such a gradient is found, another study exists quoting a non-detection.

The most extensive data to date are probably from Geisler et al. (1996), who recently re-examined the globular cluster system of M49 with deep Washington photometry, and clearly showed a color gradient. However, the gradient is rather due to a different mixture of two populations in the inner and outer parts than to a steady increase of metallicity to the center as interpreted by authors in the past.

The gradient in M49 is of the order of 0.4 Δ[Fe/H]/$\Delta logR$. This would translate into 0.06 $\Delta(V-I)/\Delta logR$ according to our relation of Sect. 4.1, or $\Delta(V-I)$ = 0.12 to 0.16 mag over the range studied in our cases. We are therefore clearly not sensitive enough to detect such gradients in our data, and can only exclude gradients as large a 0.15 $\Delta(V-I)/\Delta logR$ (or 1.0 $\Delta[Fe/H]/\Delta logR$) for our galaxies. One would need very good photometry a couple of magnitudes deeper in a sensitive system (e.g. Washington or B and I Johnson-Cousins, Geisler et al. 1996) to find gradients, if present, in the globular cluster systems studied here.

Bridges et al. (1991) found a decrease of 0.2 mag in $B-V$ from 1′ to 3′ of the center in NGC 1399. Over this range, the increase might also exists in our data, but is smaller than the scatter and can in no case be extrapolated further out.

An interesting characteristic of the globular clusters in NGC 1399 might be noticed: the large dispersion of colors derived in Sect. 4.2 exists at all radii, as in the case of M49 (Geisler et al. 1996).

5. Spatial distributions

5.1. The angular distributions

We looked for any anisotropic distribution of globular clusters around NGC 1374, NGC 1379, NGC 1387, and NGC 1427. No deep image centered on NGC 1399 was available. We computed the counts in the same rings as for the GCLFs (i.e. excluding the centers, and out to 120″). We devided the ring in 16 × 22.5 degrees segments around NGC 1374, NGC 1379, NGC 1387, and NGC 1427, and plotted the distributions modulo π, (i.e. rotating the western side by 180 degrees around the center to increase a possible excess along a given axis) in Fig. 8. For NGC 1374 and NGC 1427 (E1 and E3 galaxies respectively), we indicated the position angle of the galaxies with dotted lines. The amount of background contamination in a segment is shown as a solid line.

All the distributions are compatible with the globular clusters being spherically distributed around the galaxy. In NGC 1374 a 2σ excess of objects along the major axis of the galaxy is present. For NGC 1427 it can be excluded that the globular cluster system is as elliptical as the galaxy. For NGC 1379 (E0), the distribution with an ellipticity of 0.2 ± 0.1 and a position angle of 70 ± 10 degrees fits the data equally well as a spherical distribution.

5.2. The radial distributions

5.2.1. The “normal” galaxies

For NGC 1374, NGC 1379, NGC 1387, and NGC 1427 we computed the surface density profile for all objects found around the galaxy down to V = 24.0 mag without any correction for completeness. Table 7 shows the densities computed in increasing elliptical rings 22.7″ (100 pix) wide. The density profiles are plotted in Fig. 9, the upper panel showing the uncorrected distribution, the lower panel showing the distribution corrected for background contamination (see Sect. 5.3) together with the arbitrarily shifted galaxy light profile (squares). The excess in NGC 1374 at about 150″ corresponds to the distance of NGC 1375, the smaller galaxy close in projection to NGC 1374, which might contribute a few globular clusters.

5.2.2. NGC 1399

For NGC 1399 we computed the surface density profile in the NE and NW fields individually. We counted all objects found in the fields down to V = 24.0 mag, in rings around the center

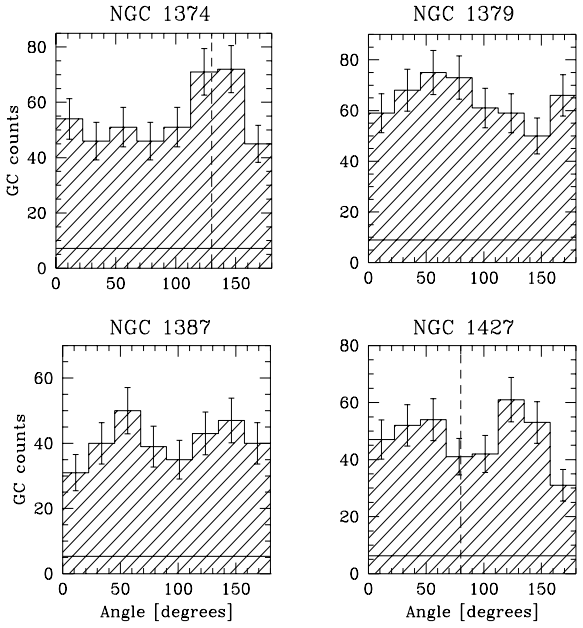

Fig. 8. The angular distributions of globular clusters around NGC 1374, NGC 1379, NGC 1387, and NGC 1427. The globular clusters were counted in 22.5 degrees wide segments around the galaxy and taken modulo π

Table 7. Density profiles for the normal galaxies. Column 1 shows the semi-major axis at the center of the ring in arcsecs, columns 2-5 the density of objects per square arcmin for our four galaxies

a	NGC 1374	NGC 1379	NGC 1387	NGC 1427
$57''$	45.4 ± 6.1	37.9 ± 5.3	33.4 ± 5.0	59.4 ± 8.0
$80''$	19.8 ± 3.1	21.4 ± 3.1	15.2 ± 2.6	21.6 ± 3.7
$102''$	12.4 ± 2.1	12.1 ± 2.0	10.2 ± 1.8	17.3 ± 2.8
$125''$	7.4 ± 1.4	6.9 ± 1.3	5.2 ± 1.1	13.8 ± 2.2
$147''$	10.6 ± 1.5	5.7 ± 1.1	5.3 ± 1.0	7.8 ± 1.5
$170''$	4.0 ± 0.9	7.0 ± 1.2	3.6 ± 0.8	10.1 ± 1.7
$193''$	6.4 ± 1.0		4.1 ± 0.8	11.4 ± 1.9
$216''$	5.4 ± 0.9		4.0 ± 0.8	9.4 ± 1.7
$238''$	3.5 ± 0.7		6.2 ± 1.0	6.2 ± 1.4
$261''$	4.0 ± 1.1		4.4 ± 1.1	6.6 ± 1.4

of the galaxy, $22.7''$ (100 pix) wide, and corrected the counts for geometrical incompleteness, i.e. we computed the fraction of the ring seen in the field, and scaled the counts up to the total area. No correction for completeness of the counts was necessary, since for NGC 1399 the counts were almost complete down to the considered magnitude. The background contamination was determined with a background field located about 40 arcmin east. The background field needed a small ($< 5\%$) correction for completeness to be adjusted to the fields around NGC 1399. The result gave 361 objects on 59.0 square arcmin in the background field down to $V = 24$ mag, or a background density of 6.1 ± 0.3 objects per square arcmin as background value for the counts in both fields around NGC 1399. Table 8 shows the densities computed in increasing elliptical rings $22.7''$ (100 pix) wide, plotted in Fig. 10.

Table 8. The density profile of globular clusters around NGC 1399. Column one list the mean ring radii, column 2 and 3 show the density of objects found in the NE and NW field

radius	NGC 1399 NE	NGC 1399 NW
$57''$	89.7 ± 18.7	83.4 ± 8.6
$80''$	49.7 ± 10.1	34.5 ± 5.8
$102''$	43.8 ± 7.9	40.2 ± 5.7
$125''$	38.5 ± 6.4	43.1 ± 5.4
$147''$	32.0 ± 5.3	26.8 ± 4.0
$170''$	24.5 ± 4.2	25.2 ± 3.6
$193''$	20.6 ± 3.6	19.7 ± 3.0
$216''$	14.2 ± 2.8	14.0 ± 2.4
$238''$	22.3 ± 3.3	12.4 ± 2.2
$261''$	15.3 ± 2.6	11.4 ± 2.0
$284''$	16.0 ± 2.5	13.5 ± 2.1
$307''$	12.1 ± 2.1	10.2 ± 1.8
$329''$	12.2 ± 2.0	11.5 ± 1.8
$352''$	10.7 ± 1.8	11.3 ± 1.8
$375''$	11.2 ± 1.8	8.1 ± 1.4
$397''$	13.2 ± 1.9	8.2 ± 1.4
$420''$	9.3 ± 1.6	8.0 ± 1.4
$443''$	8.8 ± 1.5	8.8 ± 1.4
$465''$	9.7 ± 1.5	8.4 ± 1.7
$488''$	6.7 ± 1.3	6.0 ± 1.7
$511''$	6.5 ± 1.5	9.5 ± 2.4
$534''$	5.9 ± 1.6	6.9 ± 2.3
$556''$	4.8 ± 1.6	8.6 ± 3.0

5.3. Globular cluster system vs. galaxy profiles

For NGC 1399, we fitted a power-law of the kind $\rho \sim r^{-x}$, where ρ stands for the surface density of the globular clusters or the surface intensity of the galaxy light respectively, and r for the semi-major axis, of both the globular cluster density profile and the light of the galaxy (taken from our isophotal models, see Sect. 2.2, all in good agreement with similar data from Goudfrooij et al. 1994). For the four other galaxies we solved for the slope and the background density ρ_{bkg} simultaneously by fitting a function of the kind $\rho = a \cdot r^{-x} + \rho_{bkg}$ as proposed by Harris (1986), when the data do not reach reliably the background level. The resulting coefficients are shown in Table 9. The results agree with the data from Hanes & Harris (1986) who found all profiles compatible with a slope of -2, and for NGC 1399 with the profile from Wagner et al. (1991), who found a slope of -1.54 ± 0.15 for the globular cluster density profile, and -1.67 ± 0.12 for the galaxy light. All density profiles of the globular clusters follow the galaxy light within the uncertainties. But in NGC 1399 the clearly flatter globular cluster density profile only agrees with the light profile due to the large cD envelope of the galaxy (e.g. Schombert 1986).

For the four normal galaxies, the values found are very similar to results of previous studies of globular cluster systems

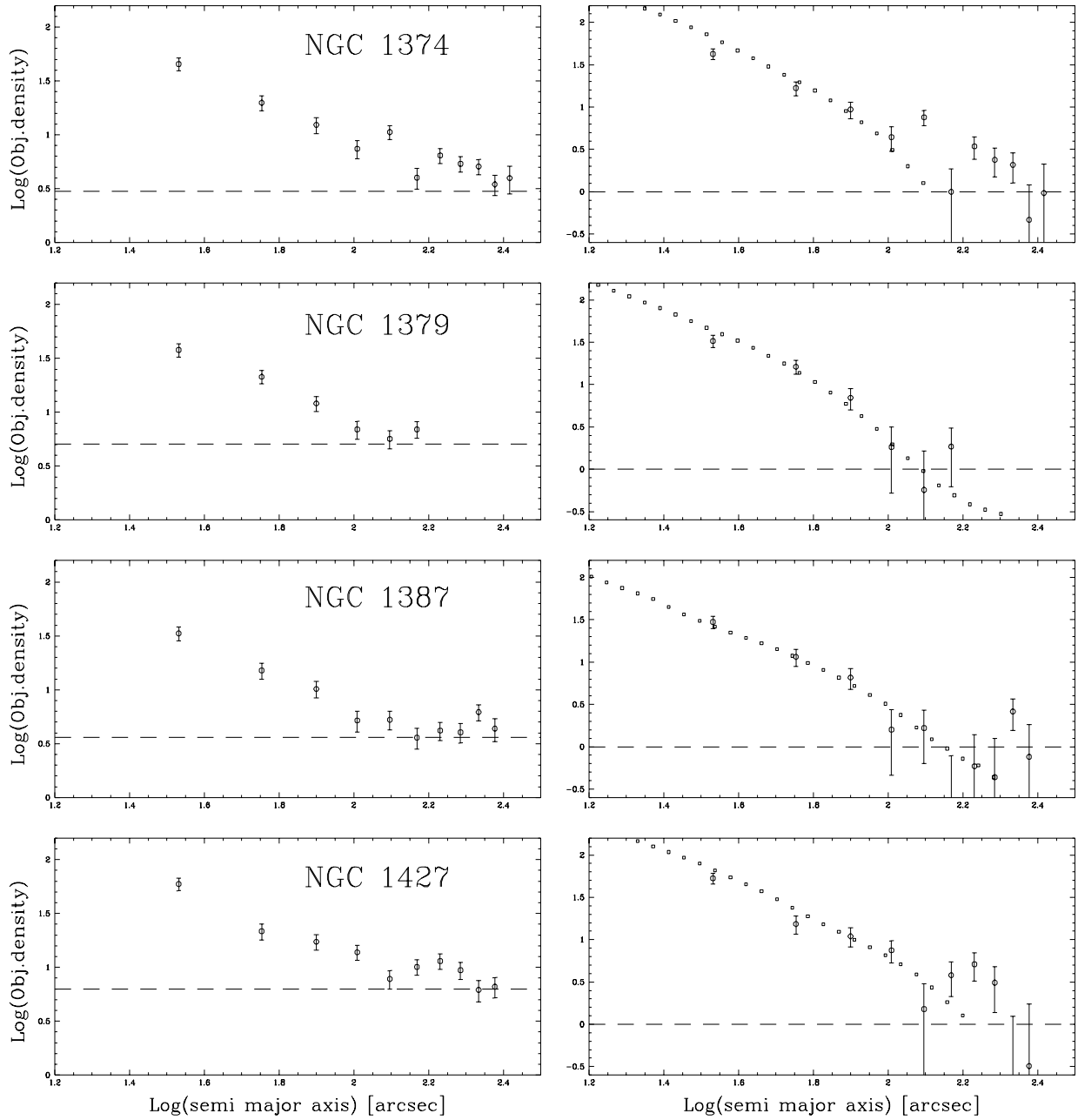

Fig. 9. The radial distribution of objects in NGC 1374, NGC 1379, NGC 1387, and NGC 1427. The left and right panels respectively show the uncorrected density profile and the density profile corrected for background contamination together with the arbitrarily shifted galaxy light profile (squares). Surface densities are given in number per square arcminute

around normal early-type galaxies (e.g. Kissler-Patig et al. 1996 and references therein).

6. Discussion

The previous sections demonstrate that while the globular cluster systems of our faint early-type galaxies have very similar properties, the globular clusters in NGC 1399, the central giant elliptical cD galaxy, are much more numerous and have a different color distribution as well as a flatter density profile.

While it is true for NGC 1399 that globular clusters appear in a much larger number than in spirals, it is not for our fainter galaxies. Harris & Harris (1996) compiled all the globular cluster systems investigated to date. If we select from their list all the S0, Sa, and Sb galaxies (excluding the two outstanding galaxies with $M_V < -22$), we get for the ten remaining galaxies an average number of globular clusters of 345 ± 185 per galaxy, for an average luminosity of $M_V = -21.1$. The three ellipticals and the S0 galaxy that we investigated here have a mean

Table 9. Slope coefficients for the globular cluster density (column 2) and galaxy light (column 3) of our target galaxies (column1), as well as the fitted background (column 4)

Galaxy name	density slope	gal. light slope	bkg density
NGC 1374	1.8 ± 0.3	2.0 ± 0.1	3.0 ± 2.0
NGC 1379	2.1 ± 0.6	2.2 ± 0.1	5.1 ± 2.1
NGC 1387	2.2 ± 0.3	2.2 ± 0.1	3.6 ± 0.8
NGC 1427	2.0 ± 0.3	1.8 ± 0.1	6.3 ± 1.7
NGC 1399 NE	1.55 ± 0.25	1.75 ± 0.10	(6.1 ± 0.3)
NGC 1399 NW	1.75 ± 0.30	1.75 ± 0.10	(6.1 ± 0.3)

of 406 ± 81 globular clusters and therefore do not have more globular clusters in absolute numbers than do these spirals.

Comparing the specific frequencies of spirals to that of ellipticals is very difficult, if it makes sense at all. First because ideally it should relate the number of globular clusters to the mass of the galaxy by assuming a constant M/L ratio, which is a reasonable assumption when comparing ellipticals among each other but not when comparing spirals with ellipticals. Second because even when reducing this discrepancy by normalizing the number of globular clusters to the spheroid luminosity, it is unclear which fraction of the globular clusters in spirals are associated with the halo and the bulge, while elliptical galaxies are most probably bulge dominated. Thus it is not clear if we compare comparable values. However, as a comparison, the sample of spirals mentioned above has an average S of 1.3 ± 0.8, and would S be computed for the spheroid luminosities, it would increase by about 1 (e.g. Harris 1991). The value for spirals does therefore not deviate that much from the values derived in Sect. 3.2.

Similarity seems to exist further in the color distribution of the globular clusters in our faint galaxies and in spirals. They are slightly redder (i.e. probably more metal-rich), but show a similar dispersion around the median to that in the Milky Way, and cover a similar range of colors. Here again dominating bulge clusters, in contrast to the halo dominated Milky Way system, could possibly explain the small color differences.

Finally we conclude that for our faint elliptical galaxies there is no strong need to a different globular cluster formation or evolution scenario, as well as no need for any increase of the number of globular clusters during a hypothetic merger event.

On the contrary, for NGC 1399 these conclusions are not true. NGC 1399 has far more globular clusters, and a much higher specific frequency than the spiral galaxies. The surface density profile is much flatter and the globular clusters cover rather homogeneously the full range of colors, and show signs of several populations. As pointed out by several authors before, the formation of the globular cluster system in NGC 1399 must have undergone a different history, similar to other central giant ellipticals (e.g. Harris 1991). Note that the globular cluster system of NGC 1399 confirms all the predictions that Ashman & Zepf (1992) made for a globular cluster system that experienced a merger: it has a broad (multi-modal?) color distribution, a flat surface density profile, and an increased number of globular clusters. However, NGC 1399 is one of the galaxies

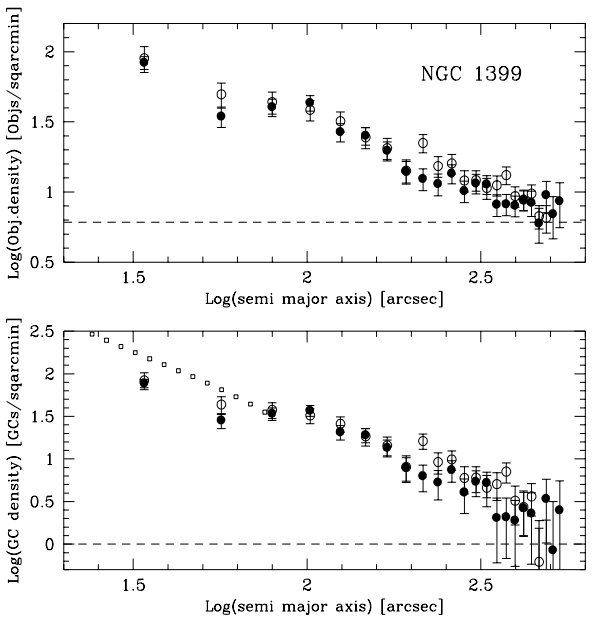

Fig. 10. The radial distribution of objects in NGC 1399. The symbols are the same as in Fig. 9

with an outstanding specific frequency, even for a possible enrichment by a merger. While the formation of a large number of globular clusters in cooling flows seems to be ruled out (Bridges et al. 1996), it was speculated that NGC 1399's position in the center of the Fornax cluster favored the huge number of globular clusters also observed in other galaxies lying at the center of galaxy clusters (e.g. Harris 1991). One possibility would be the increased number of merger events at early times, since we showed that the multi-modal color distribution does not exclude *several* components to have formed the globular cluster system of NGC 1399. Another hypothesis could be that the large number of globular clusters is related to the large number of dwarf galaxies whose density Hilker et al. (1995) reported to increase significantly towards the center of the Fornax cluster. One could speculate that accreted while still gaseous, the dwarf galaxies formed with high efficiency globular clusters in the dense environment of NGC 1399. The high specific frequency would then be a consequence of a Searle & Zinn (1978) scenario combined with the dense environment of NGC 1399. However, no more than speculations could be made to date to explain the high specific frequencies of central galaxies.

Finally we note the constancy of the specific frequencies in all our faint galaxies. The mean for our faint early-type galaxies in Fornax is 4.2 with a dispersion of 1.0. We can add NGC 1404, another probable member of Fornax from a study of Richtler et al. (1992, however note their possible argument against a membership of the galaxy to the cluster), and assume a similar distance modulus of 31.0 ± 0.2. We then get a absolute magnitude of -21.0 ± 0.2, and a specific frequency of 3.5 ± 0.8. The effectiveness in globular cluster formation within the normal galaxies of the Fornax galaxy cluster must have been very similar and

might hint to similar formation histories of the galaxies in the cluster.

Acknowledgements. We wish to thank the staff of the Las Campanas observatory for the friendly atmosphere and their valuable help during the observing run. Thanks also to Bill Harris for providing a electronic copy of his globular cluster system compilation, and later for his comments as referee that helped to improve the paper. MKP acknowledges a studentfellowship at the European Southern Observatory, SK and MH were supported by the DFG project Ri 418/5-1, LI would like to acknowledge support from *Proyecto* FONDECYT # 1960414, and HQ from *Proyecto* 1960413. HQ also acknowledges the award of a 1995 Presidential Chair in Science. This research made use of the NASA/IPAC extragalactic database (NED) which is operated by the Jet Propulsion Laboratory, Caltech, under contract with the National Aeronautics and Space Administration.

References

Aguilar L., Hut P., Ostriker J., 1988, ApJ 335, 720
Ashman K.M., & Zepf S.E., 1992, ApJ 384, 50
Ashman K.M., Bird C.M., Zepf S.E., 1994, AJ 108, 2348
Bridges T.J., Hanes D.A., Harris W.E., 1991, AJ 101, 469
Bridges T.J., Carter D., Harris W.E., Pritchet C.J., 1996, MNRAS in press
Burstein D., Heiles C., 1982, AJ 87, 1165
Conti P.S., Vacca W.D., 1994 ApJ 423, L97
Couture J, Harris W.E., Allwright J.W.B., 1990, ApJS 73, 671
Couture J, Harris W.E., Allwright J.W.B., 1991, ApJ 372, 97
Geisler D., Forte J.C., 1990, ApJ 350, L5
Geisler D., Lee M.G., Kim E., 1996, AJ 111, 1529
Goudfrooij P., Hansen, L., Jorgensen H.E., et al., 1994, A&AS 104, 179
Hanes D.A., Harris W.E., 1986, ApJ 309, 564
Harris W.E., 1986, AJ 91, 822
Harris W.E., 1991, ARA&A 29, 543
Harris W.E., 1995, in "Stellar Populations", IAU Symp. 164, eds. P.C. van der Kruit & G. Gilmore, Dodrecht: Kluwer, p.85
Harris W.E., 1996, electronically published catalog, Mc Master University
Harris H.C.,& Harris W.E., 1996, Astrophysical Quantities, 4th ed., in press
Hilker M., Kissler-Patig M., Richtler T., Infante L., 1995, AG Abstr.Series 11, 222
Hilker M., Kissler-Patig M., 1996, A&A 314, 357
Holtzman J.A., Faber S.M., Shaya E.J., et al., 1992, AJ 103, 691
Kissler-Patig M., Richtler T., Hilker M., 1996 A&A 308, 704
Kohle S., Kissler-Patig M., Hilker M., et al. , 1995, A&A 309, L37 (Paper I)
Landolt A.U., 1992, AJ 104, 340
Lee M.G., Geisler, D., 1993, AJ 106, 493
Lutz D., 1991, A&A 245, 31
Ostrov P., Geisler D., Forte J.C., 1993, AJ 105, 1762
Poulain P., 1988, A&AS 72, 215
Poulain P., Nieto J.-L., 1994, A&AS 103, 573
Richtler T., Grebel E.K., Domgörgen H., Hilker M., Kissler M., 1992, A&A 264, 25
Richtler T., 1995, in "Reviews of Modern Astronomy", Vol.8, eds. G. Klare, Springer, p.163
Schombert J.M., 1986, ApJS 60, 603
Schweizer F., Seitzer P., 1993, ApJ 417, L29
Searle L., Zinn R., 1978, ApJ 225, 357
Secker J., Geisler D., McLaughlin D.E., Harris W.E., 1995, AJ 109, 1019
Taylor B.J., 1986, ApJS 60, 577
Tully R.B., 1988, Nearby Galaxies Catalog, Cambridge University Press
Van den Bergh S., 1990, in Dynamics and Interactions of Galaxies, ed. R.Wielen (Berlin:Springer), 492
Wagner S., Richtler T., Hopp U., 1991, A&A 241, 399
Whitmore B.C., Schweizer F., Leitherer C., Borne K., Robert C., 1993, AJ 106, 1354
Whitmore B.C., Schweizer F., 1995, AJ 109, 960
Zepf S.E., Ashman K.M., Geisler D., 1995, ApJ 443, 570

This article was processed by the author using Springer-Verlag LaTeX A&A style file *L-AA* version 3.